Fabrication of Metal Nanoparticles by Pulsed Laser Ablation in Supercritical CO_2

Motonobu Goto[1]*, Siti Machmudah[1], Wahyudiono[2], Armando T. Quitain[2] and Mitsuru Sasaki
[1] Bioelectrics Research Center, Kumamoto University, Kurokami 2-39-1, Kumamoto 860-8555, JAPAN
[1] Graduate School of Science and Technology, Kumamoto University, Kurokami 2-39-1, Kumamoto 860-8555, JAPAN

E-mail: mgoto@kumamoto-u.ac.jp; Fax: +81-96-342-3665

Abstract

Fabrication of nano-structured materials has been developed by performing pulsed laser ablation of copper, gold, and silver plates in supercritical CO_2. The metal nano-structured particles were successfully generated with allowing the selective generation of clusters. Laser ablation was performed with an excitation wavelength of 532 nm. On the basis of the experimental result, both surface of ablated metal plates and structure of nanoparticles were significantly affected by the changes in supercritical CO_2 density. The deepest crater was created near the critical pressure of CO_2. As increasing irradiation time, plume deposited in the surrounding crater created by the ablation was clearly observed. In FE-SEM image of the generated gold nano-structured particles on silicon wafer, a network structure of smaller gold particles was fabricated. The network structure consists of gold nanoclusters with an average diameter of approximately 30 nm in ensembles of 300-800 nm length. The difference morphology of particles fabricated from silver plate was observed. Based on the results, this new method can also be used to obtain advanced nano-structured materials.

Keyword: pulsed laser ablation, supercritical CO_2, gold nanoparticles, silver nanoparticles

INTRODUCTION

Pulsed laser ablation (PLA) has become a promising method of the synthesis of nanoclusters for photonics, electronics and medicine [1–9]. The PLA method has several advantages compared to more traditional techniques. In particular, it was shown that this method provides a possibility for chemically clean synthesis, which is difficult to achieve under more conventional nanoparticle production conditions. In addition, several experimental studies indicated that the cluster size distribution could be controlled in PLA by carefully choosing the laser irradiation parameters and properties of the background gas. Furthermore, laser ablation allows for an easy production of colloidal metal nanoparticles for biological and medical applications.

Fabrication of nanoparticles under laser ablation of solids either in gas or in vacuum has been extensively explored during the last decade. Formation of nanoparticles under laser ablation of solids in liquid environment has been studied to a much lower extent. Formation of both gold (Au) and silver (Ag) nanoparticles under ablation of corresponding solids by

pulsed Nd:YAG laser has been reported recently [10–15]. Formation of Ag-Au alloy under radiation of a second harmonic of Nd:YAG laser has been observed [16].

The possibility of ablation in pressurized and supercritical CO_2 environment has been demonstrated recently [17, 18]. CO_2 under supercritical condition is an interesting fluid with critical temperature (31^oC) close to the ambient and an easily achieved critical pressure of 7.4 MPa. Compared with liquids, the higher diffusivity in supercritical fluid allows increased reaction rates when the diffusion limitations are great. Having a zero surface tension, the supercritical fluid allows complete penetration into metal cavity. Furthermore, the lower viscosity of supercritical fluid in comparison with the liquids can reduce the solvent-cage effects and therefore increase the initiator efficiency. Since the solvent power of supercritical fluid is directly related to its density, a large variation in solubility can be achieved by simply changing the pressure and temperature of the system. Moreover, by simple pressure reduction, phase change is observed, and the supercritical fluid is transformed to a gas and exits the system without leaving any residues.

Silicon nanoclusters and gold nanonecklaces have been observed by performing PLA in supercritical CO_2 [17, 18]. However, the investigation of PLA under pressurized and supercritical CO_2 condition has not been much published yet. The phenomenon of ablation in pressurized and supercritical CO_2 has not clearly understood yet. The aim of the present work is to examine the characterization of ablated copper, gold and silver plates and to investigate the fabrication of gold and silver nanoparticles under PLA in pressurized and supercritical CO_2 environment.

MATERIALS AND METHODS

Materials

Copper, gold and silver plates with thickness of 1 mm used for PLA target and silicon wafer for collecting the fabricated gold and silver nano-structured particles were purchased from Nilaco, Japan. CO_2 was obtained from Uchimura Co., Japan.

Methods

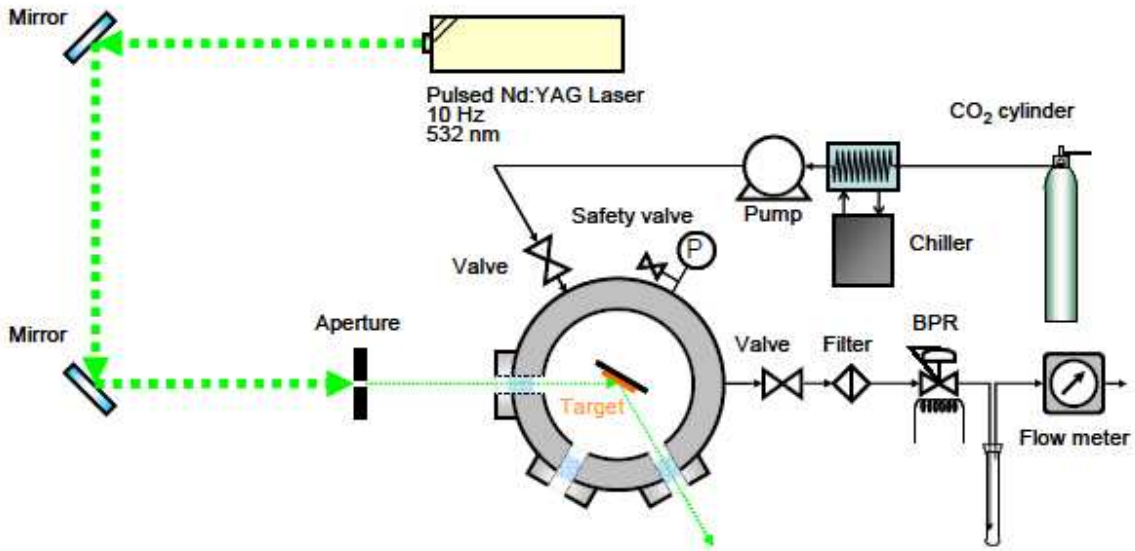

Figure 1 Schematic diagram of experimental apparatus of PLA with a high pressure cell

PLA was carried out in a high-pressure cell (SUS 316, 110 ml volume, AKICO, Japan) with three sapphire windows. The schematic diagram of the experimental apparatus is shown in **Figure 1**. The second harmonic of a Q-switched pulsed Nd:YAG laser (Spectra-Physics Quanta-Ray INDI-40-10, wavelength: 532 nm, pulse energy: maximum 200 mJ/(cm2.pulse), pulse duration: 8 ns, repetition frequency: 10 Hz) was used. Target was fixed in a high-pressure cell. Incident angle of the laser beam was 30^{o} and the laser was located 1 m from the target. Copper, gold or silver plate (Nilaco, purity: 99.99%, thickness: 1 mm, 1x1 cm) was used as the target. Liquid CO_2 was pressurized and pumped into the cell using a high-performance liquid chromatography (HPLC) pump (Jasco PU-1586). A silicon wafer was placed perpendicular with the target, to collect gold and silver nanoparticles. The cell temperature was controlled by a temperature controller at constant temperature of 40^{o}C. The pressure of the system was varied from 0.1 to 20 MPa. After the setting temperature and pressure were reached, PLA was performed for 5000 s. The laser beam was collimated by a 1-mm-diameter of aperture without any focusing lens. The surface morphology of the target after ablation and the crater depth after PLA were observed by laser scanning microscopy (Keyence, VK-9510). Gold and silver nanoparticles generated on the silicon wafer were performed by FE-SEM (Hitachi, SU8000) and characterized by fast Fourier transformation (FFT). The particle size distribution of generated nanoparticles was determined by Image J software.

RESULTS

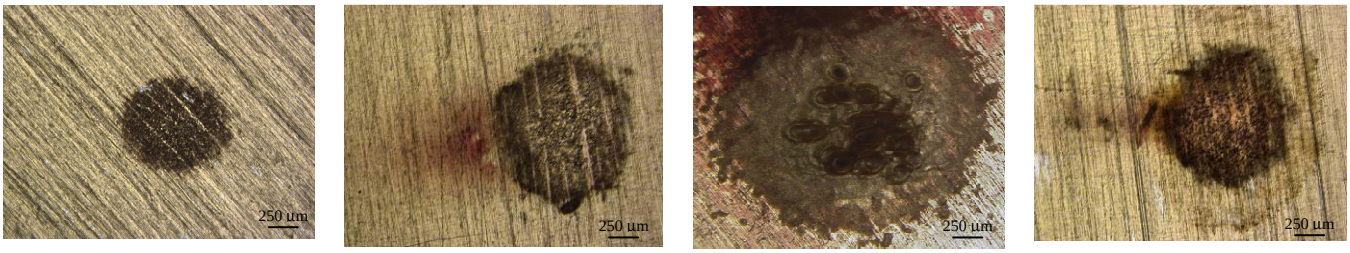

(a) (b) (c) (d)

Figure 2 Laser scanning microscopy image of gold plate after ablation at 40^{o}C for 3000s by Nd:YAG laser. (a) in air at ambient pressure; (b) in liquid CO_2 at 5.5 MPa; (c) in $scCO_2$ at 10 MPa; (d) in $scCO_2$ at 20 MPa

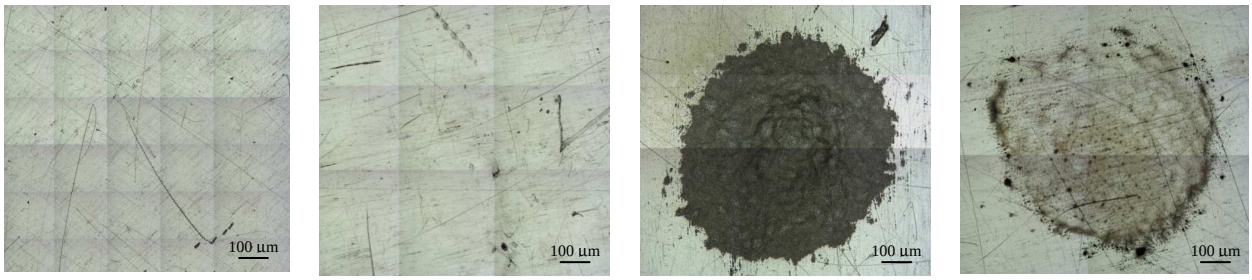

(a) (b) (c) (d)

Figure 3 Laser scanning microscopy image of Ag plate after irradiation at 40^{o}C for 5000s by Nd:YAG laser. (a) in CO_2 at 0.2 MPa; (b) in CO_2 at 5 MPa; (c) in $SCCO_2$ at 7 MPa; (d) in $SCCO_2$ at 20 Mpa

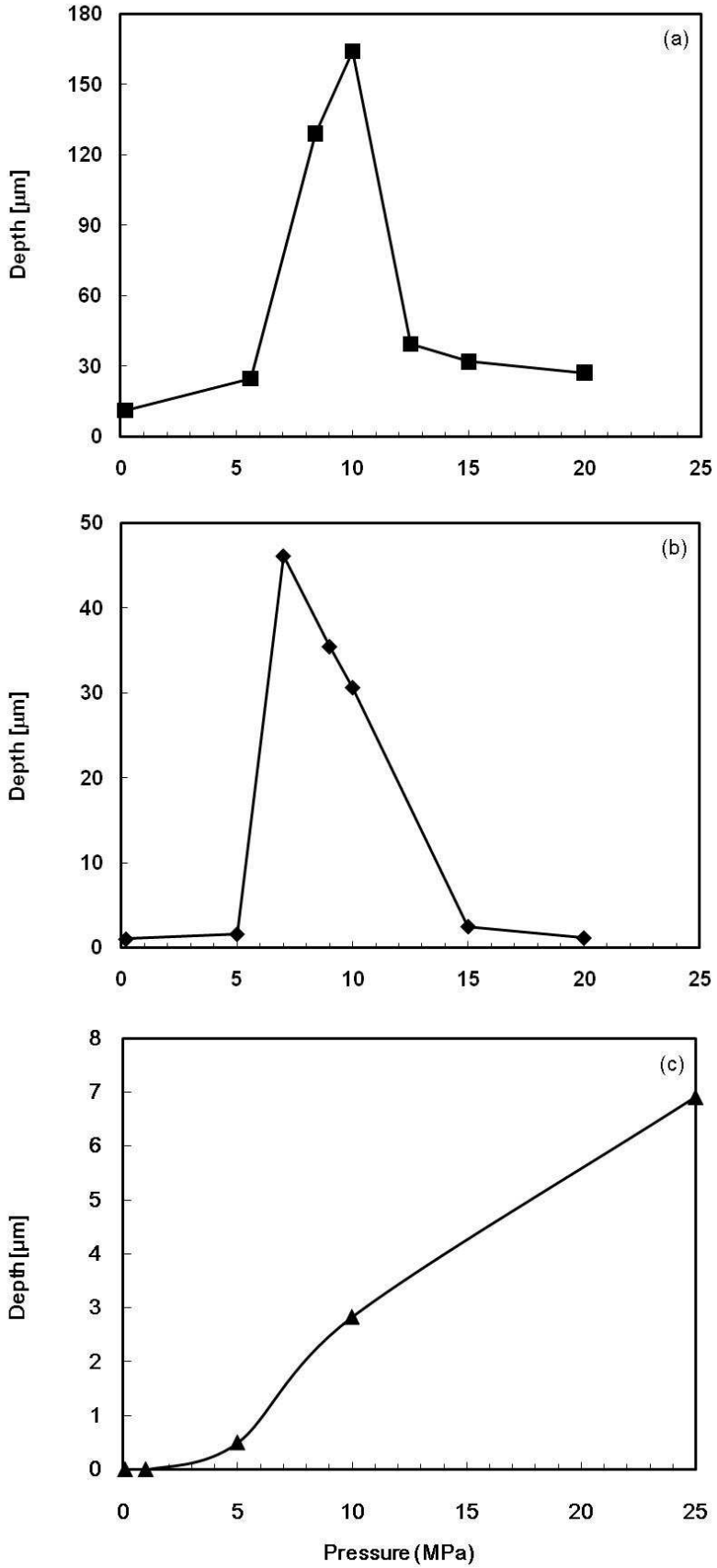

Figure 4 Depth of crater generated by PLA on the gold (a), silver (b) and copper (c) plates

Characterization of irradiated copper, gold and silver plates was performed by surface morphology observation and measurement of crater depth using laser scanning microscopy. On the basis of observation, an ellipse crater was generated on the surface of copper, gold and silver plates. As shown in **Figure 2** and **3** for the image of ablated gold and silver plates, respectively, at low CO_2 pressure up to 5.5 MPa, the crater could not be observed clearly on the surface both gold and silver of plates. However, the crater was clearly generated as increasing pressure, especially at 10 and 7 MPa for gold and silver plates, respectively. The width and depth of crater also increased at this condition. In addition, the surface around irradiation area was slightly rough due to the accumulation of solid particles deposition (debris). In the ablation of metal plate, the metals melted and then ejected nano-structured particles. Some nano-structured particles were still remained on the plates due to deposition of metal particles during the ablation process. It has been explained that the metal vapor produced by laser is rapidly quenched just above the metal surface in the pressurized surrounding medium [16]. The particles deposition spreads in a circular zone around the crater. The diameter of debris deposition in a circular zone around the irradiated craters was found to increase with increasing CO_2 pressure. However, the deepest crater and the widest debris deposition were observed at 10 and 7 MPa of PLA in $SCCO_2$ for ablated gold and silver plates, respectively.

On the basis of laser scanning microscopy image, the crater depth generated by PLA was determined. **Figure 4(a)**, **(b)** and **(b)** show the pressure dependency of crater depth generated by PLA on the gold, silver and copper plates, respectively, at 40^{o}C and 5000 s. At the same condition, crater generated on the gold plate was deeper than that on the copper and silver plates. The melting point of gold (1064^{o}C) is higher than that of silver (961^{o}C), however the latent heat of fusion and specific heat of gold (65 J/g and 129 J/K.kg, respectively) are lower than that of silver (103 J/g and 237 J/K.kg). It indicates that gold needs smaller heat to raise the temperature during a melting process than silver at same laser fluence. Thus, it caused faster ablation on gold plate than that on silver plate.

In **Figure 4(a)** and **(b)**, the crater depth on both gold and silver plates increased with increasing pressure up to a certain pressure and then decreased with an increase in pressure. The deepest crater was observed at near critical pressure of CO_2 (7.4 MPa). At this condition, a number of physical and chemical properties of CO_2 are commonly intermediate between gas and liquid states. It has been reported that the fluid local structure in the vicinity of a molecule changes from a gas-like to a liquid-like structure at around a density of $\rho r = 0.7$ (pressure of 6.18 MPa). The local structure of the supercritical fluid changes the degree of aggregation or the cooling rate of hot atoms in the fluid, which plays an important role in determining the generation processes of nanoclusters [17]. Because of the change of local structure of ablation medium with the existence of metal vapor, the maximum point of ablation process might change for both gold and silver targets. In the case of maximum crater depth, the deepest craters of gold and silver plates were obtained at 10 and 7 MPa, respectively. The pressures are relatively close to the critical pressure of CO_2. Thermal conductivity of CO_2 at 10 and 7 MPa are 6.8×10-2 and 2.8×10-2 J/h.m.K, respectively, while the calculation of time constant [19] of gold (205 nm particle mean diameter) at 10 MPa and silver (52 nm particle mean diameter) at 7 MPa for heat transport from the target to CO_2 are 4 and 2.3 ns, respectively. These time constants are smaller than 8 ns of pulse duration used in this work. It indicates that it is possible to transfer the heat from the target to CO_2 during the short pulse duration of 8 ns. In addition, it also evidenced that high thermal conductivity of CO_2 gave positive effect to the ablation process. In this case, higher thermal conductivity of CO_2 did not only result in higher heat transfer from the target to the medium, but also resulted in higher thermal transfer from

laser to the target; and as the result deeper crater was created. Even though thermal conductivity of CO_2 increases with an increase in pressure, higher pressure caused decreasing crater depth. It might be related to the dense surrounding medium of the target. The higher pressure indicates the denser surrounding medium. Thus, the layer adjacent to the laser exposed area of the target becomes thicker and the laser was difficult to penetrate the layer. Therefore, the laser fluence decreased when it reached the metal; and resulted in shallow crater. In addition, both crater depths of gold and silver plates may be related to the constant volume heat capacity of CO_2. Constant volume heat capacity of CO_2 increases with increasing pressure up to the critical pressure, then decreases with increasing pressure. This characteristic is similar with both crater depths of gold and silver plates.

On the contrary, the depth of ablated copper plate increased as increasing pressure. It might be due to the increasing CO_2 density at high pressure. The higher density of supercritical CO_2 is conjectured to suppress deposition of particles generated from the ablated surface of the copper plate due to dispersion in supercritical CO_2. In fact, no debris or particles were observed, but only an undulation was observed in the center of the ablated crater on the Cu plate surface. In particular, the density increases remarkably and its value at 25 MPa is several tens or hundreds of times higher than that at 0.1 MPa. Since the ablation efficiency at high pressure is also several tens or hundreds of times greater than at low pressure, laser ablation in high-pressure supercritical CO_2 can be assumed to be influenced by the CO_2 density.

Typical FE-SEM image of the gold and silver nanoparticles on the silver wafer is shown in **Figure 5(a)** and **(b)**, respectively. The ablation was carried out at 40^oC and 10 MPa for gold and 7 MPa for silver. The conditions were maximum points of ablation for the metals. The morphology of both gold and silver particles was basically sphere-like structure. The gold particles contain relatively larger-sized gold nanoparticles with larger-varied diameter ranging from 5 to 1000 nm (**Figure 6(a)**). In **Figure 5(a)**, bigger gold nanoparticle is surrounded by network structure of smaller-sized gold nanoclusters in ensembles of 300-800 nm length. The network structure of gold nanoclusters may modify the properties of gold nanoparticles. Unfortunately, the absorption spectrum of the particles was not measured in this work. The attached gold nanoclusters on the gold nanoparticles may occur due to the fast coagulation and quenching of the gold atoms in the dense CO_2 environment. The medium adjacent to the laser-exposed area of the target contains a significant amount of gold nanoclusters, which favors their growth and the formation of network structure [16]. As observation on the FE-SEM image, gold nanoclusters were also spread on the silver wafer (**Figure 5(a)**).

In the ablation of silver plate, neither the size nor shape changed. The formation of silver nanoparticles was different from the gold nanoparticles. Silver particles contain larger-sized silver nanoparticles with larger-varied diameter ranging from 3 nm to 1.2 μm (**Figure 6(b)**). Bigger silver nanoparticles melted during the ablation process and then ejected smaller spherical silver nanoparticles, which surrounded the molten silver nanoparticles (**Figure 5(b)**). The smaller silver nanoparticles were also spread on the silicon wafer.

Moreover, FFT was also performed on the FE-SEM image of single gold and silver nano-sphere particles (inset of **Figure 5(a)** and **(b)**, respectively). The FFT images of both gold and silver particles show glowing bright spots arranged in a systematic pattern, indicating that each nanoparticle is a single crystal composed of parallel crystallographic planes. The FFT images also indicate that nanoparticles growth directions are parallel and perpendicular [20].

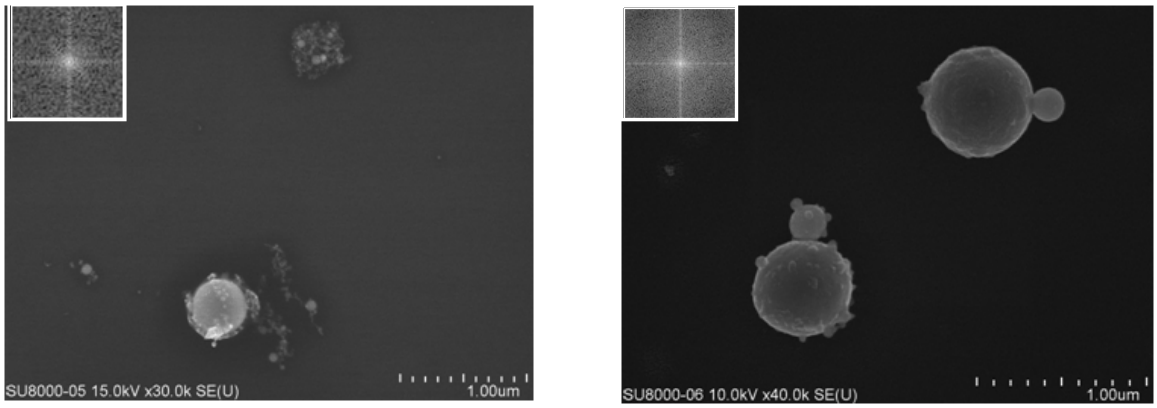

(a) (b)

Figure 5 FE-SEM image of gold (a) and silver (b) nanoparticles generated by PLA at maximum PLA condition

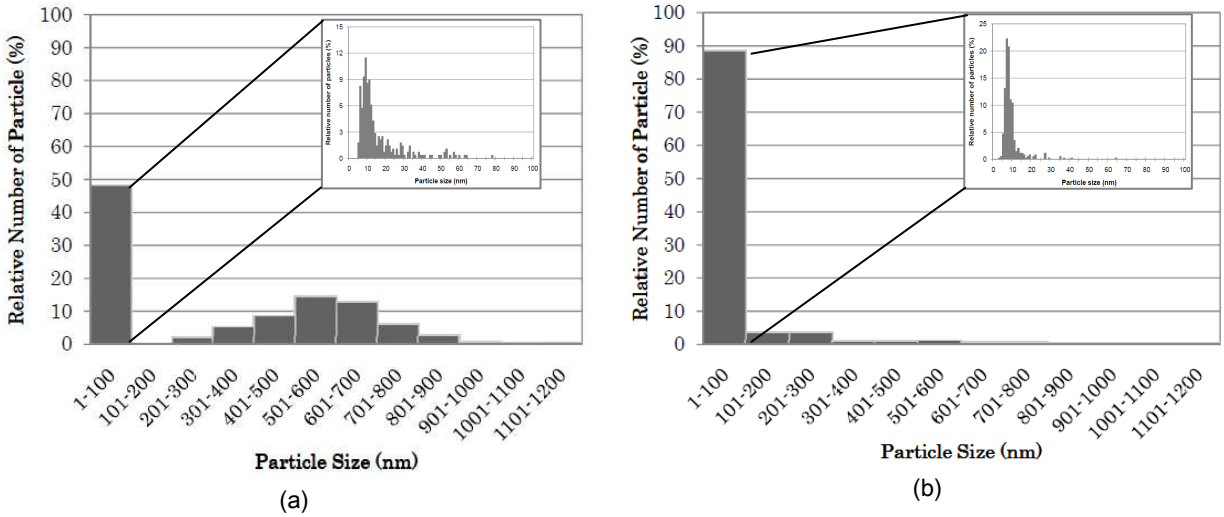

(a) (b)

Figure 6 Particle size distribution of gold (a) and silver (b) nanoparticles generated by PLA at maximum PLA condition

CONCLUSION

Fabrication of gold and silver nanoparticles has been carried out by PLA under supercritical CO_2 condition. The morphology of ablated gold and silver plates and fabricated Gold and silver nanoparticles were reported. The crater depth of gold and silver plates had correlation with constant volume heat capacity of CO_2 as the PLA medium. The fabricated gold particles contain relatively larger-sized gold nanoparticles with larger-varied diameter ranging from 5 to 1000 nm. Moreover, the fabricated silver particles contain larger-sized silver nanoparticles with larger-varied diameter ranging from 3 nm to 1.2 μm.

ACKNOWLEDGEMENT

This work was supported by Kumamoto University Global COE Program “Global Initiative Center for Pulsed Power Engineering”, Grant-in-Aid for Scientific Research by Ministry of Education, Culture, Sports, Science and Technology, Japan, and Japan Society for the Promotion of Science (JSPS). Authors would like to thank to Dr. K. Shigemori at Kumamoto Industrial Research Institute for analysis assistant of laser microscopy.

REFERENCES :

[1] MOVTCHAN, I. A., DREYFUS, R.W., MARINE, W., SENTIS, M., AUTRIC, M., Le Lay, G., Thin Solid Films, Vol. 255, **1995**, p. 286.
[2] MAKIMURA, T., MIZUTA, T., MURAKAMI, K., Appl. Phys. Lett., Vol. 76, **2000**, p. 1401-1403.
[3] MOVTCHAN, I.A., MARINE, W., DREYFUS, R.W., LE, H.C., SENTIS, M., AUTRIC, M., Appl. Surf. Sci., Vol. 96, **1996**, p. 251.
[4] GEOHEGAN, D.B., PURETZKY, A.A., DUSHER, G., PENNYCOOK, S.J., Appl. Phys. Lett., Vol. 72, **1998**, p. 2987.
[5] PATRONE, L., NELSON, D., SAFAROV, V.I., SENTIS, M., MARINE, W., GIORGIO, S., J. Appl. Phys., Vol. 87, **2000**, p. 3829.
[6] MARINE, W., PATRONE, L., LUK’YANCHUK, B., SENTIS, M., Appl. Surf. Sci., Vol. 154–155, **2000**, p. 345-352.
[7] OZEROV, I., NELSON, D., BULGAKOV, A., MARINE, W., SENTIS, M., Appl. Surf. Sci., Vol. 212–213, **2003**, p. 349.
[8] ALBERT, O., ROGER, S., GLINEC, Y., LOULERGUE, J.C., ETCHEPARE, J., BOULMER-LEBORGNE, C., PERRIERE, J., MILLON, E., Appl. Phys. A: Mater. Sci. Process., Vol. 76, **2003**, p. 319.
[9] SCUDERI, D., BENZERGA, R., ALBERT, O., REYNIER, B., ETCHEPARE, J., Appl. Surf. Sci., Vol. 252, **2006**, p. 4360.
[10] SIBBALD, M. S., CHUMANOV, G., COTTON, T. M., J. Phys. Chem., Vol. 100, **1996**, p. 4672.
[11] KAMAT, P.-V., FLUMIANI, M., HARTLAND, G.V., J. Phys. Chem. B, Vol. 102, **1998**, p. 3123.
[12] TAKAMI, A., KURITA, H., KODA, S., J. Phys. Chem. B, Vol. 103, **1999**, p. 1226.
[13] LINK, S., BURDA, C., NIKOOBAKHT, B., EL-SAYED, M.A., J. Phys. Chem. B, Vol. 104, **2000**, p. 6152.
[14] ABID, J.-P., GIRAULT, H.H., BREVET, P.F., Chem. Commun., Vol. 9, **2001**, p. 829.
[15] DOLGAEV, S.I., SIMAKIN, A.V., VORONOV, V.V., SHAFEEV, G.A., BOZON-VERDURAZ, F., Appl. Surf. Sci., Vol. 186, **2002**, p. 546.
[16] SIMAKIN, A.V., VORONOV, V.V., SHAFEEV, G.A., BRAYNER, R., BOZON-VERDURAZ, F., Chem. Phys. Lett., Vol. 348, **2001**, pp. 182.
[17] SAITOW, K., J. Phys. Chem. B, Vol. 109, **2005**, p. 3731.
[18] SAITOW, K., YAMAMURA, T., MINAMI, T., J. Phys. Chem. C, Vol. 112, **2008**, p. 18340.
[19] WILSON, O.M., HU, X., CAHILL, D.G., BRAUN, P.V., Phys. Rev. B, Vol. 66, **2002**, p. 224301-(1-6).
[20] PHURUANGRAT, A., THONGTEM, T., THONGTEM, S., Mater. Lett., Vol. 63, **2009**, p. 1562.